ISSN 1674-1056
http://cpb.iphy.ac.cn
http://iopscience.iop.org/cpb
中国物理 B
Chinese Physics
中国物理
Chinese Physics B

Effect of particle size distribution on magnetic behavior of nanoparticles with uniaxial anisotropy

S Rizwan Ali, Farah Naz, Humaira Akber, M Naeem, S Imran Ali, S Abdul Basit, M Sarim, Sadaf Qaseem

Citation: Chin. Phys. B . 2018, 27(9): 097503. **doi:** 10.1088/1674-1056/27/9/0975

Journal homepage: http://cpb.iphy.ac.cn; http://iopscience.iop.org/cpb

What follows is a list of articles you may be interested in

Typicality at quantum-critical points

Lu Liu(刘录), Anders W Sandvik, Wenan Guo(郭文安)

Chin. Phys. B . 2018, 27(8): 087501. **doi:** 10.1088/1674-1056/27/8/087501

Radio-frequency-heating capability of silica-coated manganese ferrite nanoparticles

Qiu Qing-Wei, Xu Xiao-Wen, He Mang, Zhang Hong-Wang

Chin. Phys. B . 2015, 24(6): 067503. **doi:** 10.1088/1674-1056/24/6/067503

Composite magnetic nanoparticles：Synthesis and cancer-related applications

Cai Ping, Chen Hong-Min, Xie Jin

Chin. Phys. B . 2014, 23(11): 117504. **doi:** 10.1088/1674-1056/23/11/117504

Using magnetic nanoparticles to manipulate biological objects

Liu Yi, Gao Yu, Xu Chenjie

Chin. Phys. B . 2013, 22(9): 097503. **doi:** 10.1088/1674-1056/22/9/097503

Magnetic nanoparticle-based cancer therapy

Yu Jing, Huang Dong-Yan, Muhammad Zubair Yousaf, Hou Yang-Long, Gao Song

Chin. Phys. B . 2013, 22(2): 027506. **doi:** 10.1088/1674-1056/22/2/027506

Effect of particle size distribution on magnetic behavior of nanoparticles with uniaxial anisotropy

S Rizwan Ali[1,†], Farah Naz[1], Humaira Akber[1], M Naeem[1],
S Imran Ali[2], S Abdul Basit[3], M Sarim[3], and Sadaf Qaseem[1]

[1] *Department of Physics, Federal Urdu University of Arts, Science and Technology, Karachi, Pakistan*
[2] *Department of Applied Chemistry and Chemical Technology, University of Karachi, Karachi, Pakistan*
[3] *Department of Computer Science, Federal Urdu University of Arts, Science and Technology, Karachi, Pakistan*

(Received 10 April 2018; revised manuscript received 29 June 2018; published online 28 August 2018)

The effect of particle size distribution on the field and temperature dependence of the hysteresis loop features like coercivity (H_C), remanence (M_R), and blocking temperature (T_B) is simulated for an ensemble of single domain ferromagnetic nanoparticles with uniaxial anisotropy. Our simulations are based on the two-state model for $T < T_B$ and the metropolis Monte–Carlo method for $T > T_B$. It is found that the increase in the grain size significantly enhances H_C and T_B. The presence of interparticle exchange interaction in the system suppresses H_C but causes M_R to significantly increase. Our results show that the parameters associated with the particle size distribution ($D_{d,\delta}$) such as the mean particle size d and standard-deviation δ play key roles in the magnetic behavior of the system.

Keywords: magnetic nanoparticles, Monte Carlo simulations, size distribution, interparticle interaction, hysteresis

PACS: 75.50.Tt, 75.40.Mg, 75.60.Ej **DOI:** 10.1088/1674-1056/27/9/097503

1. Introduction

With the technological advancements in the field of magnetic recording, size effects on the magnetic properties of nanostructures including spherical particles, nanodots, nanowires, nanopillars, and thin films become increasingly important.[1–3] Single domain magnetic nanoparticles of Co, Ni, FePt, etc. with high anisotropy and magnetic moment are of particular importance.[4–6] In order to attain higher recording densities with these materials, their grain size has to be small.[7] Smaller grains undergo thermally activated magnetization reversals, resulting in the loss of recorded information. However, the magnetization of small particles can be effectively stabilized against thermal fluctuations by inducing additional anisotropy in the system, e.g., exchange bias in core-shell nanoparticles[8] or by using shape anisotropy.[9] Better understanding of size related effects in magnetic nanoparticles is the key to designing and optimizing thermally stable high density recording media. For these systems, not only is the mean particle size of relevance but also the broadness in the size distribution, because the presence of very small grains results in partial thermal instabilities whereas very large grains may enhance the coercivity (H_C) from a medium to an intolerable limit. Studies have shown the significance of grain size for the thermal stability of the magnetization of fine particles[10,11] but broadness in the particle size distribution has not been explicitly studied. Xu *et al.*[12] have shown that the shape of the hysteresis loop for non-interacting spherical particles in dilute random composites is indeed sensitive to the broadness of the size distribution.

Here, we consider a system of spherical particles having a Gaussian size distribution. These particles are assumed to be single domain with uniaxial anisotropy axes randomly distributed in space. We study the effect of broadness in the size distribution on the field and temperature dependence of magnetization by using a two-state model and the metropolis Monte Carlo (MMC) method. Magnetic properties such as the H_C and blocking temperature (T_B) are found to be very sensitive to size variations, whereas remanence (M_R) is found to be largely independent of the broadness of the particle size distribution. We also simulate the effects of interparticle exchange interaction on the magnetic behavior of these particles. Our results show a decrease in H_C and increase in M_R of the system with increasing strength of exchange interaction. The rest of this paper is organized as follows. In Sections 2 and 3, we deal with the description of the model system and theoretical framework within which we perform the simulations. In Section 4, we present our results followed by the discussion of some important aspects of our results. Finally, in Section 5 we draw some conclusions from the study of this work.

2. Model system

First, we consider a system of 1200 non-interacting nanoparticles which are assumed to be well-dispersed in a nonmagnetic matrix. These particles have a Gaussian size-distribution ($D_{d,\delta}$) with d as the average diameter (2 nm, 3 nm, and 4 nm) and δ as the standard deviation (1 nm, 1.5 nm,

†Corresponding author. E-mail: rizwan@fuuast.edu.pk
© 2018 Chinese Physical Society and IOP Publishing Ltd

and 2 nm). Physically, δ corresponds to the dispersion or broadness in the distribution of particle size. The effects of d and δ are systematically studied for five samples with different $D_{d,\delta}$, viz., $D_{2,1}$, $D_{3,1}$, $D_{4,1}$, $D_{4,1.5}$, and $D_{4,2}$. Initially, we consider a system with low packing density such that the interparticle interactions can be ignored. This allows us to test our model system within the theoretical framework of the Stoner–Wohlfarth (SW) model.[13,14] The atomic moments within each nanoparticle are assumed to be uniformly oriented so that their resultant moment can be treated as a point dipole located at the center of the particle. Each particle has uniaxial anisotropy with anisotropy constant $K_1 \sim 1.0 \times 10^6$ J/m^3, which is slightly greater than that of bulk fcc Co.[15,16] The measurement time τ_m is kept consistent with the experimental value, i.e., 100 s.[17] Finally, we extend this model to the case where the effects of interparticle exchange interaction are taken into consideration. Here, the simulations are run for different relative exchange strength values (J/k) ranging from 0 to 0.4, where J is the exchange energy and $k = K_1V$ is the anisotropy energy barrier of a particle of volume V. In the experimental measurements, the value of J is generally not defined.[18] Thus, in our simulations we treat it as a free parameter and its value is taken to be volume dependent.

3. Simulations

We use a quasi static process in our MMC simulations in which the energy of the system is evaluated at each change in the external parameter. The moments are reoriented on the basis of energy minimum criteria. Figure 1 shows a schematic representation of our model system. The Hamiltonian of the system as suggested by the SW model is given by[19–21]

$$E = K_1V\sin^2(\theta_o - \theta) - \mu H\cos\theta, \tag{1}$$

where θ_o is the angle between the easy axis and the applied magnetic field H, and θ is the angle between the moment μ and the applied magnetic field (Fig. 1). For each particle, μ is defined by its V and specific magnetization M_o (taken as 1.43×10^6 A·m^{-1} for Co). In general, the state of each particle is described by the temperature T of the system and τ_m. Keeping τ_m constant, T_B of the particles is given by

$$T_B = K_1V/k_B\ln(\tau_m/\tau_o), \tag{2}$$

where k_B is the Boltzmann constant, K_1V is the energy barrier height in the absence of applied field, and τ_o is the characteristic relaxation time ($\sim 10^{-9}$ s).[22,23] Here, T over T_B defines the state of the system. For $T < T_B$, the particles are in a blocked state and possess pure ferromagnetic features, which can be simulated by the two-state model. In this model, there is a finite probability that the moment may switch between the two energy minimum states. Numerical calculations[24] have shown that E_B is a function of K_1V and H and is expressed as

$$E_B(H) = K_1V(1 - H/H_A)^\gamma, \tag{3}$$

where H_A is given by $2K_1h_S/M_o$ and $\gamma = 0.86 + 1.14h_S$, whereas h_S is defined by $h_S(\theta_o) = [(\cos\theta_o)^{2/3} + (\sin\theta_o)^{2/3}]^{-3/2}$.[23] For each particle, the orientation of its moment is driven by the interplay between its local H_C and applied H,[23] where $H_C = 0.48\ H_A(1 - (T/T_B)^{0.77})$. For the low applied field, i.e., $H < H_C$, the process of magnetization reversal is simulated by calculating the transition probability from one minimum to the other by using $p = 1 - \exp(-\tau_m/\tau)$, where τ is the characteristic reversal time of the moments. On the other hand, at elevated temperatures, i.e., $T > T_B$, the particles are in a superparamagnetic (SPM) state and the orientation of their moments is governed by the MMC technique.[22]

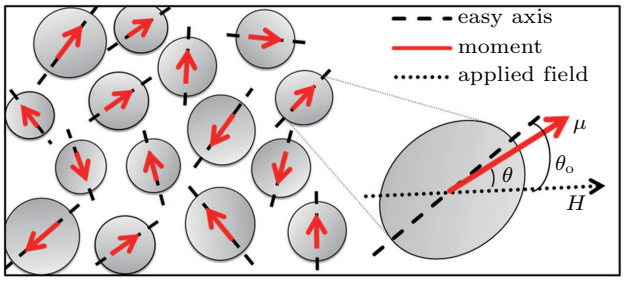


Fig. 1. (color online) Schematic representation of the system of nanoparticles with random orientation of the moment (left). Angle distribution showing the direction of moment, field, and easy axis (right).

4. Results and discussion

Figure 2 shows some representative $M(H)$ loops simulated at different temperatures for the sample with size distribution $D_{4,1}$. The initial state of the system is defined by setting $H = 0$. In this state, all the moments are distributed evenly in state 1 and state 2, thus giving zero net magnetization of the system. At small H, some of the moments, mainly those associated with smaller particles start switching to the state corresponding to the field direction. With increasing H in small steps, the moments keep on aligning with H and the magnetization gradually approaches to its saturation value M_s, when all the moments align with H. These initial magnetization processes are similar to each other for all distributions and are omitted in the hysteresis loops (± 1 T) of the samples. In the descending field branch, the magnetization follows a different path and reaches a remenant state having the value of M_R as H decreases from 1 T to 0. It should be noted that the sample exhibits strong M_R at 10 K. The higher values of M_R at low temperature are attributed to small thermal energy (k_BT) which is not sufficient for the moments to undergo thermally activated reversals even at $H = 0$. Thus, at low temperature, all the moments remain blocked in the ferromagnetic state. When H is applied in the reverse direction, the

moments start to switch from their random and blocked state and align with the reverse field. This results in a decrease in M/M_s until it vanishes near $H = -H_C$. The further increase in the field aligns all the moments along the reverse field direction and the magnetization achieves $-M_s$. The same process continues for the ascending field branch of the $M(H)$ loop. At 50 K (down triangles), some of the smaller particles become SPM, i.e., their moments become thermally unstable and start to fluctuate between their minimum energy states. The large M_R present in this loop is attributed to the fact that the fraction of small sized SPM particles is not very large at 50 K. With increasing temperature, the fraction of thermally unstable particles increases and accounts for the observed decrease in M_R and H_C. Near 190 K, all the particles become SPM and their magnetization loop can be described by the Langevin function. In the SPM regime, k_BT overcomes the Zeeman and anisotropy energies and the moments undergo fast switching between their minimum energy states, i.e., $M = 0$ at $H = 0$.

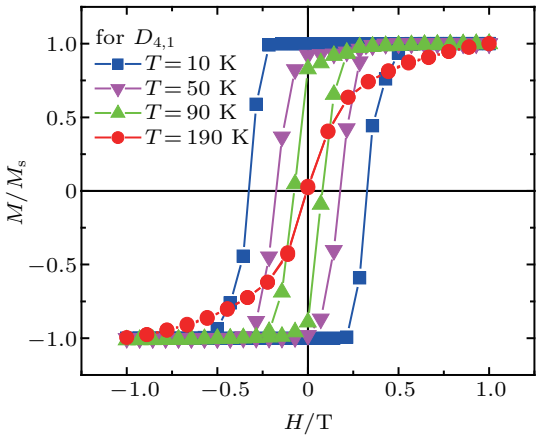


Fig. 2. (color online) Variations of M/M_s with H for the sample with size distribution $D_{4,1}$ at different temperatures.

Figure 3 shows the effect of temperature on H_C for samples with different $D_{d,\delta}$. For all samples, H_C is found to be large at very low temperature and decreases with increasing temperature. Here, we have two different cases. Case 1: for the samples with constant d (4 nm), i.e., for samples $D_{4,1}$, $D_{4,1.5}$, and $D_{4,2}$. In this case, the values of H_C are found to be the same for all samples at 10 K (Fig. 3(a)). This is attributed to the same value of d for each sample. Beyond 10 K, the value of H_C decreases sharply down to the mean T_B (100 K), which corresponds to the value of d of the sample. The rapid decrease in H_C is attributed to the increasing fraction of SPM particles due to temperature driven de-blocking transitions in the sample. Above 100 K, the decay rate of H_C becomes relatively gradual before it vanishes at a temperature which corresponds to T_B^{max}(T_B of the largest particle in the distribution). Case 2: for the samples with constant δ (1 nm), i.e., for samples $D_{2,1}$, $D_{3,1}$, and $D_{4,1}$, the temperature dependence of H_C is shown in Fig. 3(b). Overall, it is similar to the one observed for the samples in case 1. However, in contrast to case 1 (Fig. 3(a)), all the samples of case 2 exhibit different values of H_C at 10 K. Moreover, due to different values of d, each sample exhibits a different mean T_B. The value of T_B^{max} for sample $D_{2,1}$ is found to be 41 K, which is in agreement with the one observed by Xu *et al.*[12] for a system of nanoparticles having a uniform diameter of 3 nm. For the samples $D_{3,1}$ and $D_{4,1}$, we observe the large values of H_C at 10 K. This is because these samples contain particles which are larger than the largest particle present in sample $D_{2,1}$. At higher temperature, H_C for both types of samples (case 1 and case 2) vanishes at their corresponding T_B,which is consistent with the results of Du *et al.*[25] It is evident from these results that the increase in either d or δ leads to enhanced T_B for the sample.

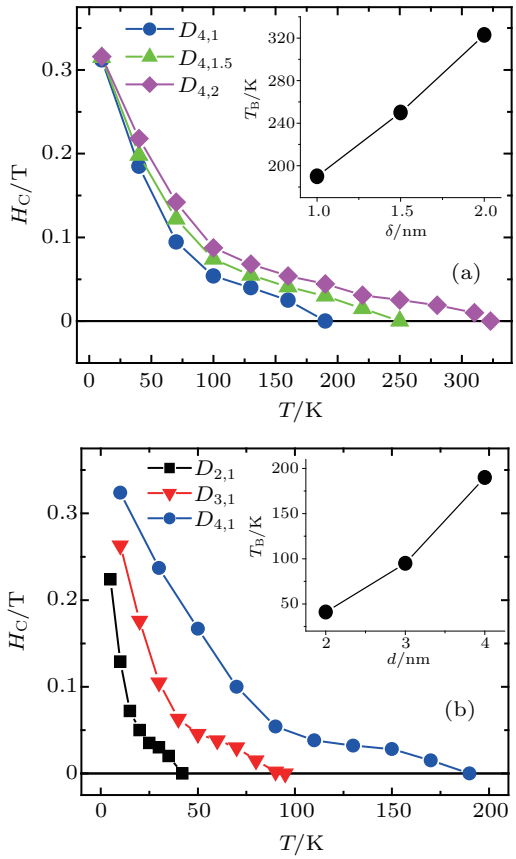


Fig. 3. (color online) Coercivity H_C as a function of temperature for distributions (a) $D_{4,1}$, $D_{4,1.5}$, $D_{4,2}$ and (b) $D_{2,1}$, $D_{3,1}$, $D_{4,1}$.

For a better understanding of the effects of particle size distribution on H_C and M_R, we compare the $M(H)$ loops of the samples with different distributions. The simulated $M(H)$ loops for the samples with constant d (4 nm) and the ones with constant δ (1 nm) are shown in Figs. 4(a) and 4(b), respectively. It is evident that the samples with broader size distributions (δ) or with larger mean diameter (d) exhibit larger H_C. This is because large δ or d implies bigger particles in the distribution with significant volume dependent anisotropy energy. This makes their moments more stable against thermal

fluctuations and external fields. A larger value of H_C is thus required to switch their direction. The value of M_R is found to be sensitive to the value of d for the sample. Thus, M_R remains largely unaltered for samples with constant d (Fig. 4(a)) whereas it decreases with decreasing value of d (Fig. 4(b)).

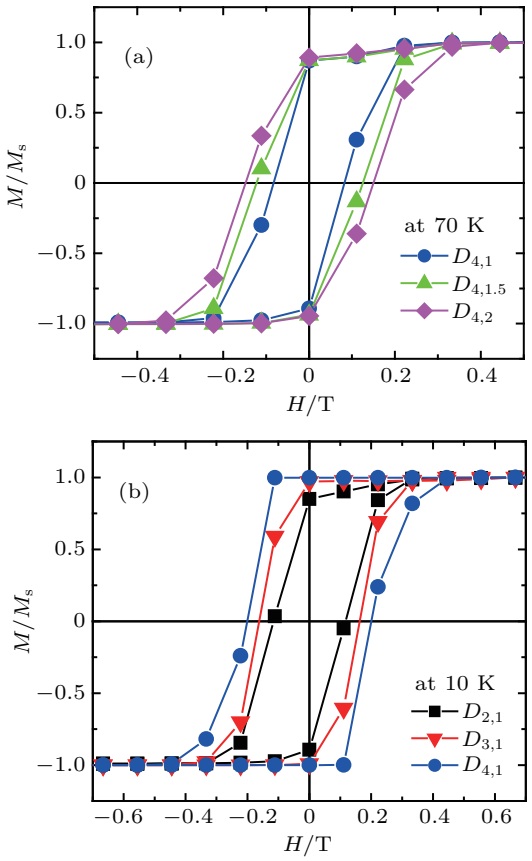


Fig. 4. (color online) Hysteresis loops $M(H)$ for distributions (a) $D_{4,1}$, $D_{4,1.5}$, $D_{4,2}$ and (b) $D_{2,1}$, $D_{3,1}$, $D_{4,1}$.

In nanoparticles, blocking/unblocking of the moments is characterized by the T_B at which zero field cooled (ZFC) magnetization $(M(T))$ passes through a maximum value. Experiments have shown that T_B depends sensitively on the particle size.[26] In order to study the effects of particle size distribution, we simulate ZFC and field cooled FC $M(T)$ for the samples with different distributions. Our ZFC (FC) process involves the cooling of the system from 300 K down to 5 K in the absence (presence) of 10 kOe field. For both ZFC and FC cases, the data are recorded during the heating of the sample from 5 K to 300 K in the presence of the field. For each sample, we observe a strong irreversibility between FC and ZFC curves, indicating the onset of the blocking transition in the samples (not shown here). Figures 5(a) and 5(b) show the simulated ZFC $M(T)$ of our samples. In all cases, the ZFC curves pass through a maximum value near the T_B of the system. This T_B corresponds to the temperature at which the particle with mean diameter (d) undergoes the blocking transition. With reducing the temperature below T_B, the particles in the ensemble undergo blocking transitions at their size dependent local T_B's. Similarly, with increasing temperature beyond T_B, the particles undergo SPM transitions. It is evident that the samples with larger δ (see Fig. 5(b)) each exhibit a rather broad ZFC peak. Additionally, with increasing values of δ and/or d, the ZFC peak shifts towards higher temperature. This behavior is consistent with the recent experimental results[27] and is attributed to the presence of larger and thermally stable particles in these samples. Thus, the size of the particles has a prominent effect on the T_B of the system: T_B increases as the size of the particles increases.

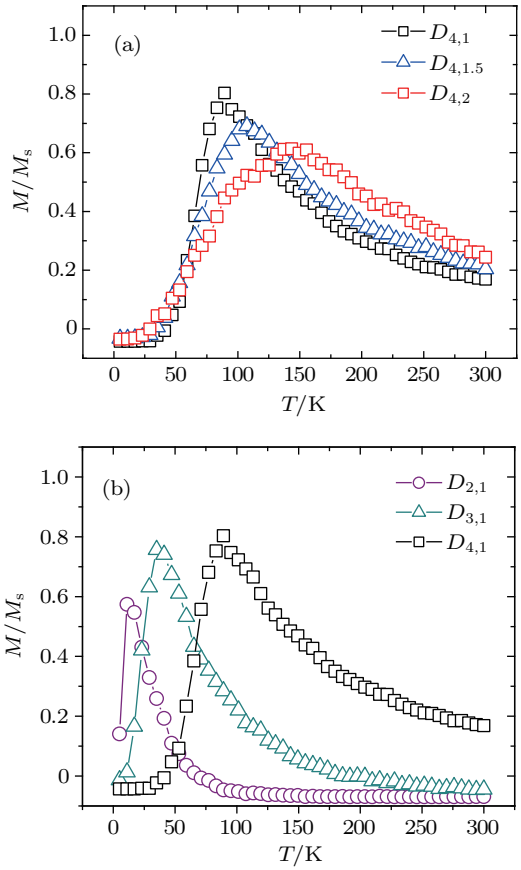


Fig. 5. (color online) Variations of M/M_s with T for distributions (a) $D_{4,1}$, $D_{4,1.5}$, $D_{4,2}$ and (b) $D_{2,1}$, $D_{3,1}$, $D_{4,1}$.

In the above discussion, we have considered systems of non-interacting nanoparticles. Next, we incorporate exchange interaction into our system. Figure 6(a) shows the effect of exchange interaction (J/k) on H_C at different temperatures. At each temperature, we observe a clear decrease in H_C with J/k increasing from 0 to 0.4. This behavior is attributed to the fact that the particles are coupled to their neighboring particles via exchange forces. If the moment of a particle undergoes switching, it can induce switching in the other particle even at a low external field.[19] This leads to suppression of H_C with increasing strength of exchange interaction. Another factor which is of interest here is the observed increase in M_R with increasing J/k for temperatures above 60 K (Fig. 6(b)). Below 60 K, M_R remains largely independent of J/k because here the thermal energy (k_BT) is too low to account for any change in M_R

at any value of J/k. Physically, J/k affects E_B of the system according to

$$E_B(H) = K_1 V (1 \pm \alpha)^2, \quad (4)$$

where $\alpha = (J + \mu H)/2K_1V$. This leads to the above mentioned changes in H_C and M_R of the system. The magnetizations are evaluated by the two-minimum approach and the results are found to be consistent with[18,28] those obtained from the system that is treated by the MMC method.

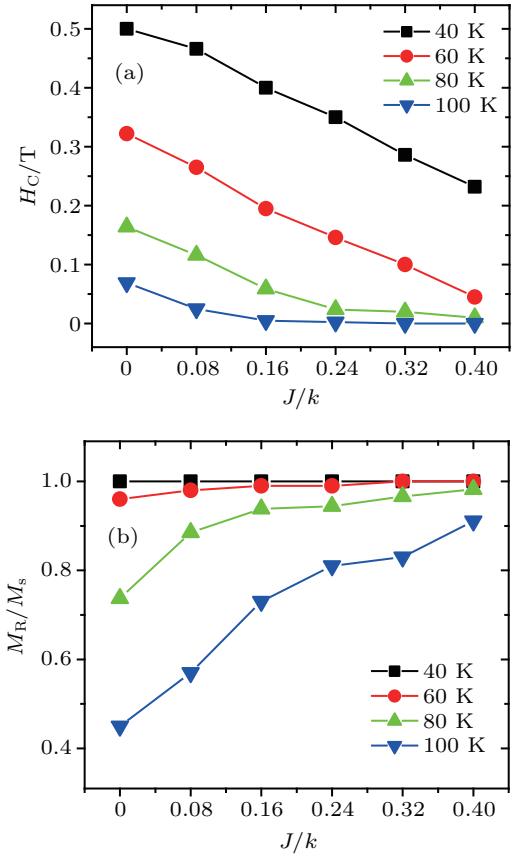


Fig. 6. (color online) Effects of exchange interaction (J/k) on (a) coercivity H_C and (b) remanence M_R/M_s at different temperatures.

5. Conclusion

The magnetic field dependence of blocking temperature and the temperature dependence of the coercive field with changing particle size distribution are studied by Monte Carlo simulations with a modified metropolis algorithm. It is found that the hysteresis curve collapses at high temperature when the particles become superparamagnetic. Thus, the shape of the hysteresis loop is found to be dependent on the particle size distribution and temperature. We also extend our model to the case where the interacting magnetic nanoparticles are taken into consideration. In this case, the coercivity decreases and remanence increases with increasing strength of the interparticle exchange interaction between the particles.

References

[1] Bedoya-Hincapie C M, Ortiz-Alvarez H H, Restrepo-Parraa E, Olaya-Florez J J and Alfonso J E 2015 *Chin. Phys. B* **24** 117701
[2] Sheng-Nan S, Chao W, Zan-Zan Z, Yang-Long H, Venkatraman S S and Zhi-Chuan X 2014 *Chin. Phys. B* **23** 037503
[3] Masrour R, Bahmad R, Benyoussef A 2013 *Chin. Phys. B* **22** 057504
[4] Wu X W, Guslienko K Y, Chantrell R W and Weller D 2003 *Appl. Phys. Lett.* **82** 3475
[5] Guimarâe Alberto P 2009 *Principles of Nanomagnetism* (Berlin: Springer Science & Business Media) p. 38 [ISBN 978-3642014819]
[6] Munoz-Sandoval E, Torres-Heredia J J and López-Urías F 2005 *J. Appl. Phys.* **97** 10
[7] Weller D and Moser A 1999 *IEEE Trans. Magn.* **35** 6
[8] Skumryev V, Stoyanov S, Zhang Y, Hadjipanayis G, Givord D and Nogués J 2003 *Nature* **423** 850
[9] Lv D L and Xu C 2010 *Chin. Phys. Lett.* **27** 097503
[10] Sánchez R D, Rivas J, Vaqueiro P, López-Quintela M A and Caeiro D 2002 *J. Magn. Magn. Mater.* **247** 92
[11] Hansen M F and Mørup S 1999 *J. Magn. Magn. Mater.* **203** 214
[12] Xu C, Li Z Y and Hui P M 2001 *J. Appl. Phys.* **89** 3403
[13] Stoner E C and Wohlfarth E P 1948 *Phil. Tran. Roy. Soc. Lond. A* **240** 599
[14] Wernsdorfer W, Orozco E B, Hasselbach K, Benoit A, Barbara B, Demoncy N, Loiseau A, Pascard H and Mailly D 1997 *Phys. Rev. Lett.* **78** 1791
[15] Bodker F, Morup S and Linderoth S 1994 *Phys. Rev. Lett.* **72** 282
[16] Respaud M 1999 *J. Appl. Phys.* **86** 556
[17] Cullity B D and Graham C D 2011 *Introduction Magn. Mater.* (Massachusetts: John Wiley & Sons) p. 425 [ISBN 978-1118211496]
[18] Kechrakos D and Trohidou K N 2003 *J. Mag. Mag. Mat.* **262** 107
[19] Aharoni A 2000 *Introduction Theory Ferromagnetism* (New York: Clarendon Press) p. 92 [ISBN 978-0198508090]
[20] Chuev M A and Hesse J 2007 *J. Phys.: Condens. Matter* **19** 506201
[21] Tannous C and Gieraltowski J 2008 *Eur. J. Phys.* **29** 475
[22] Serantes D and Baldomir D 2012 *Open Surf. Sci. J.* **4** 71
[23] Sattler K D 2011 *Handbook Nanophyscis: Nanoparticles Quantum Dots* (Boca Raton: CRC Press) p. 228 [ISBN 978-1420075441]
[24] Pfeiffer H 1990 *Phys. Status Solidi A* **122** 377
[25] Du H F and Du A 2006 *J. Appl. Phys.* **99** 104306
[26] Jaffari G H, Ali S R, Hasanain S K, Güntherodt G and Shah S I *J. Appl. Phys.* **108** 063921
[27] Chesnel K, Trevino M, Cai Y, Hancock J M, Smith S J and Harrison R G 2014 *J. Phys.: Conf. Ser.* **521** 012004
[28] Verdes C, Diaz B R, Thompson S M, R Chantrell W and Stancu A 2002 *Phys. Rev. B* **65** 174417